Fractals, Vol. 10, No. 1 (2002) 91–102

CHAOS AND STOCHASTICITY IN DETERMINISTICALLY GENERATED MULTIFRACTAL MEASURES

CARLOS E. PUENTE
Department of Land, Air and Water Resources, University of California, Davis, USA
NELSON OBREGÓN
Department of Civil Engineering, Universidad Javeriana, Bogotá, Colombia
BELLIE SIVAKUMAR
Department of Land, Air and Water Resources, University of California, Davis, USA

Received March 1, 2001; Accepted May 29, 2001

Abstract

Successful usage of a large family of deterministically generated measures to model complex nonlinear phenomena (e.g. rainfall, turbulence and groundwater contaminant transport) has been reported recently.[1–7] As these measures, generated as derived distributions of multifractal measures via fractal interpolating functions (FIF), i.e. the fractal-multifractal (FM) approach, have been found to share the inherent character of natural sets, the present study further investigates their dynamical (chaotic or stochastic) properties. It is shown, through a variety of examples and via the use of power spectrum, mass exponents and false nearest neighbors in the state-space, that the FM approach indeed generates deterministic measures whose behavior (depending on their parameters) may be classified as low-dimensional and chaotic or as high-dimensional and stochastic. These results suggest the general suitability of the FM approach for understanding and modeling nonlinear natural phenomena.

1. INTRODUCTION

A common problem in the study of irregular and apparently random natural phenomena is the assessment of whether their evolution may be understood using deterministic chaos or a stochastic approach. In practice, this involves analyzing a suitable time series associated with a phenomenon and determining the number of dominant variables necessary to allow a complete representation of its underlying dynamics.[8] If a set is dominated by a few degrees

of freedom, then a deterministic chaotic model may be suitable. On the other hand, a stochastic model may be required when a large number of dominant variables are involved.

The belief that the noticeable spatial and temporal variability of natural systems is due to the influence of a large number of variables has, in general, led researchers to employ the concept of a stochastic process to model such systems. However, research over the past two decades has resulted in a significant change in direction, as an increasing number of studies have reported successful applications of nonlinear deterministic chaotic models.

Even though a host of models, both stochastic and chaotic, have been employed throughout the years, these approaches possess certain important limitations that hamper our ability to fully describe a complex system. While the stochastic approaches often require unverifiable statistical assumptions (such as stationarity and ergodicity) and preserve only some important statistical properties of the records (rather than the records themselves), the chaotic procedures, by requiring very large and virtually noise-free time series, may often lead to misleading results.

In view of these limitations, it appears necessary to devise a new approach for modeling complex systems. Clearly, such an approach not only should overcome the aforementioned problems but also should yield outcomes that are comparable to (if not better than) the ones obtained using these approaches. To this effect, Puente[9,10] introduced a fractal-multifractal (FM) approach for modeling complex nonlinear time series (or sets over higher dimensions) as projections off fractal interpolating functions (FIF) that are "illuminated" via simple multifractal measures. As the FM approach requires neither stationarity and ergodicity nor a minimal record length, it could become a suitable methodology for modeling complex natural phenomena.

The FM approach was successfully employed to model several complex phenomena, such as rainfall,[1,3–5] turbulence,[2,3] and groundwater contamination transport.[3,6,7] The results revealed that the FM (geometric) procedure provides faithful descriptions of the above phenomena that preserve not only the classical statistical characteristics of the records but also the multifractal and chaotic properties present in them. These results also hinted at a plausible deterministic framework, via the notion of projections, for studying the dynamics of such processes.

The goal of the present study is to illustrate that the FM approach can be used to generate (deterministic) measures possessing dynamical properties similar to those reported in the literature for a variety of geophysical processes and that include, when analyzed via existing methods, both "stochastic" and "chaotic" signals. This shall be achieved considering a variety of FM measures generated from fractal functions having alternate fractal dimensions and studying their statistical and dynamical properties.

The organization of this paper is as follows. First, a brief review of the FM approach is provided, followed by a summary of the techniques used to assess whether a given series may be classified as low-dimensional and chaotic or as high-dimensional and stochastic. Then, a detailed investigation of the dynamical properties of two deterministic FM-derived measures having distinct visual character and containing 2^{16} points is provided, to show that one may be classified as chaotic and the other as stochastic. As these results are striking, the article then presents a complete sensitivity analysis of another 64 FM sets that confirm the dual dynamic nature of the deterministic measures. The article ends with a summary of the results obtained.

2. THE FRACTAL-MULTIFRACTAL APPROACH

A large number of deterministic measures (some having multifractal properties[2]) can be obtained using the FM approach.[9,10] As illustrated in Fig. 1, such measures, $DY1$ and $DY2$, are defined as derived distributions of generic multifractal measures, DX, via FIF, f_1 and f_2, i.e. $DY1 = DX \circ f_1^{-1}$ and $DY2 = DX \circ f_2^{-1}$, or, in other words, as projections over the y-axis of the measure DX lifted over the graph of an FIF.

Generic multifractal measures may be obtained following a multiplicative cascade process that divides and distributes a uniform measure (*ad infinitum*) into pieces of arbitrary sizes.[11] For instance, the binomial multiplicative measure DX shown in Fig. 1 progressively divides the uniform measure over the interval $[0, 1]$ into rectangular pieces of equal sizes containing $p_1 = 60\%$ (left) and $p_2 = 40\%$ (right) of the mass present in the previous generation.

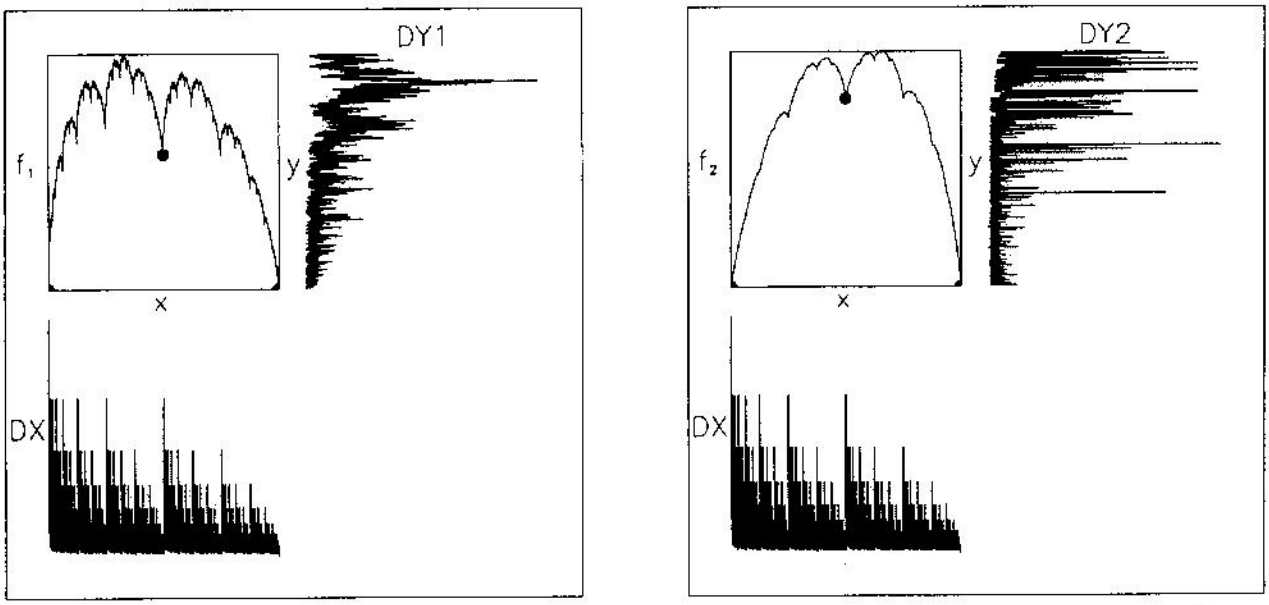

Fig. 1 Construction of deterministic FM measures *DY*1 and *DY*2. *Interpolating points*: {(0, 0), (0.5, 1), (1, 0)}; *scaling parameters*: $d_1 = 0.7$, $d_2 = 0.5$ (left), $d_1 = 0.4$, $d_2 = 0.5$ (right); *parent multifractal*: $p_1 = 0.6$, $p_2 = 0.4$.

Graphs of FIF over the plane (or in higher dimensions) are defined as unique attractors of sets of suitable affine mappings.[12,13] These are continuous functions that pass by a given set of $N+1$ points on the plane $\{(x_0, y_0), (x_1, y_1), \ldots, (x_N, y_N); x_0 < x_1 < \cdots < x_N\}$, and whose graphs may be fractal. They are obtained iterating N contractile affine mappings of the form

$$w_n\begin{pmatrix} x \\ y \end{pmatrix} = \begin{pmatrix} a_n & 0 \\ c_n & d_n \end{pmatrix}\begin{pmatrix} x \\ y \end{pmatrix} + \begin{pmatrix} e_n \\ f_n \end{pmatrix} \qquad (1)$$

such that

$$w_n\begin{pmatrix} x_0 \\ y_0 \end{pmatrix} = \begin{pmatrix} x_{n-1} \\ y_{n-1} \end{pmatrix} \qquad (2)$$

$$w_n\begin{pmatrix} x_N \\ y_N \end{pmatrix} = \begin{pmatrix} x_n \\ y_n \end{pmatrix} \qquad (3)$$

for $n = 1, 2, \ldots, N$.

The above equations imply that the parameters a_n, c_n, e_n and f_n may be obtained in terms of the coordinates of the interpolating points and the free vertical *scalings*, d_n. As (2) and (3) give $a_n = (x_n - x_{n-1})/(x_N - x_0)$ and hence $0 < a_n < 1$, for all n, the mappings w_n in (1) become contractile provided that for all n, $0 \leq |d_n| < 1$. When this condition is satisfied, a unique and, hence, deterministic "fixed-point" exists, and that is precisely the graph G of a function $f : x \to y$, which by virtue of (2) and (3) passes by the interpolating points $G = \bigcup_{n=1}^{N} w_n(G)$. The dimension $D(1 \leq D < 2)$ of the graph of an interpolating function in Ref. 13: (i) $D \geq 1$, the solution of $\Sigma|d_n|a_n^{D-1} = 1$ if $\Sigma|d_n| > 1$; and (ii) 1, if $\Sigma|d_n| \leq 1$.

Even though general analytical formulas for the derived measures are not readily available[10] (as illustrated in Fig. 1), a variety of interesting sets can indeed be obtained by varying the parameters of f and DX.[9,10] Also, additional sets may be generated by allowing projections to be calculated at an angle θ other than 90°, and by using generalized versions of the ideas to higher dimensions.[1] Depending on the nature of the FIF, the following overall behavior is found. When the fractal dimension D is close to one, derived measures of sizes similar to those found in applications turn out to have multifractal properties.[2] As D grows from one to two, the measures progressively become absolutely continuous (i.e. with a density) and in the limit they become Gaussian.[9]

As multinomial multifractals represent intermittent natural phenomena,[14,15] a descriptive physical interpretation may be advanced to the FM-derived measures as "images" or "projections" of turbulence-related phenomena. These measures become relevant in applications as they are parsimoniously encoded and as they do not exhibit geometric repetitiveness *ad infinitum*, a common objection against the use of fractal geometry.

It is important at this point to further stress some merits that the FM approach may have over the other existing methods. First, the approach is entirely deterministic, as both the parent multifractal measure and the transforming mapping may be uniquely obtained via simple recursive procedures.[10] Second, the methodology focuses on a wholistic geometric description of a given (normalized) set, rather than the preservation of relevant (multifractal) statistics, as is typically the case with other models.[16,17] Third, the approach does not rely on regularity assumptions, such as stationarity and ergodicity, as most stochastic approaches do.

3. DISTINGUISHING CHAOS AND STOCHASTICITY

The dramatic recent advances in nonlinear science and the rapidly growing set of tools for nonlinear time series analysis have brought about a major methodological revolution in studying many natural systems. Now it is known that: (1) systems can either be deterministic and chaotic or be random and unpredictable; (2) seemingly random phenomena may contain hidden structures; (3) systems may not necessarily get simpler as they are broken down; (4) infinitesimal causes can hamper our ability to predict; (5) complex systems may have simple solutions; and (6) simple equations can produce very complex behaviors. Among the large number of discoveries/theories that make up the nonlinear revolution, chaos theory has gained significant popularity in almost all fields of natural and physical sciences.

Central in a chaotic analysis of a signal is the notion of phase-space reconstruction, a topological representation of the given information via a set of suitably chosen coordinates, that allow visualizing the dynamics of a phenomenon. The physics behind such a reconstruction stems from the fact that nonlinear systems are characterized by self-interaction. Given a time series $X(t)$, $t = 1, \ldots, n$, coordinates are typically obtained using a delay time τ, so that successive m-dimensional embeddings $\mathbf{Y}_t = (X(t), X(t-\tau), \ldots, X(t-(m-1)\tau))$, $m = 2, \ldots,$ are studied.[18,19] Then, systems are classified as follows. When the signal yields stable behavior for low-dimensional representations (e.g. a fractal dimension of a strange attractor) and sensitivity to initial conditions is confirmed (i.e. via a positive Lyapunov exponent), the system in question is termed chaotic. Alternatively, when such a stable behavior is not encountered and an increasing number of coordinates are required, the phenomenon under study is classified as stochastic.

In this work, the delay time τ was defined based on the autocorrelation function[20] and on the mutual information function[21] of the records. Specifically, the number of lags to the first local minimum of such functions and the distance to a correlation equal to $1/e$[22] defined three alternative scenarios to be analyzed. In regards to the procedure used to classify the signals, the present study relies on the method of false nearest neighbors within the phase-space.[23] Such a method examines whether the attractor is properly unfolded and yields a minimum embedding dimension when the number of false nearest neighbors drops to zero.[24] Also, this procedure avoids some of the practical limitations encountered with the popular correlation dimension method.[8,25]

4. DYNAMICAL PROPERTIES OF DERIVED MEASURES *DY*1 AND *DY*2

As previously illustrated in Fig. 1, the FM procedure may be used to generate sets of arbitrary lengths that have a distinct character. This section presents a detailed dynamic analysis of sets $DY1$ and $DY2$, obtained as histograms over 2^{16} (65 536) bins in y of 800×10^6 points within the graphs of functions f_1 and f_2, as found iterating two affine mappings [Eq. (1)] using pseudo-random coin tosses with a 60–40% skew, ensuring a binomial multifractal measure DX over x.

As can be seen, $DY1$ and $DY2$, coming from functions that pass by the same set of three points $\{(0, 0), (0.5, 1), (1, 0)\}$, indeed possess different appearances and textures that reflect alternative filterings of DX as performed by functions f_1 and f_2. Since $DY1$ results from an FIF whose graph has a fractal dimension greater than one ($D = 1.263$), it integrates the parent measure and possesses much less variability than DX. As $DY2$ is found via a function that is not fractal ($D = 1$), its texture is more intermittent, for it inherits the features present in DX.

The fact that $DY1$ and $DY2$ are distinct may be further appreciated calculating some of their statistics. As shown on the top of Fig. 2, both signals are fairly complex as they exhibit power-law scaling on

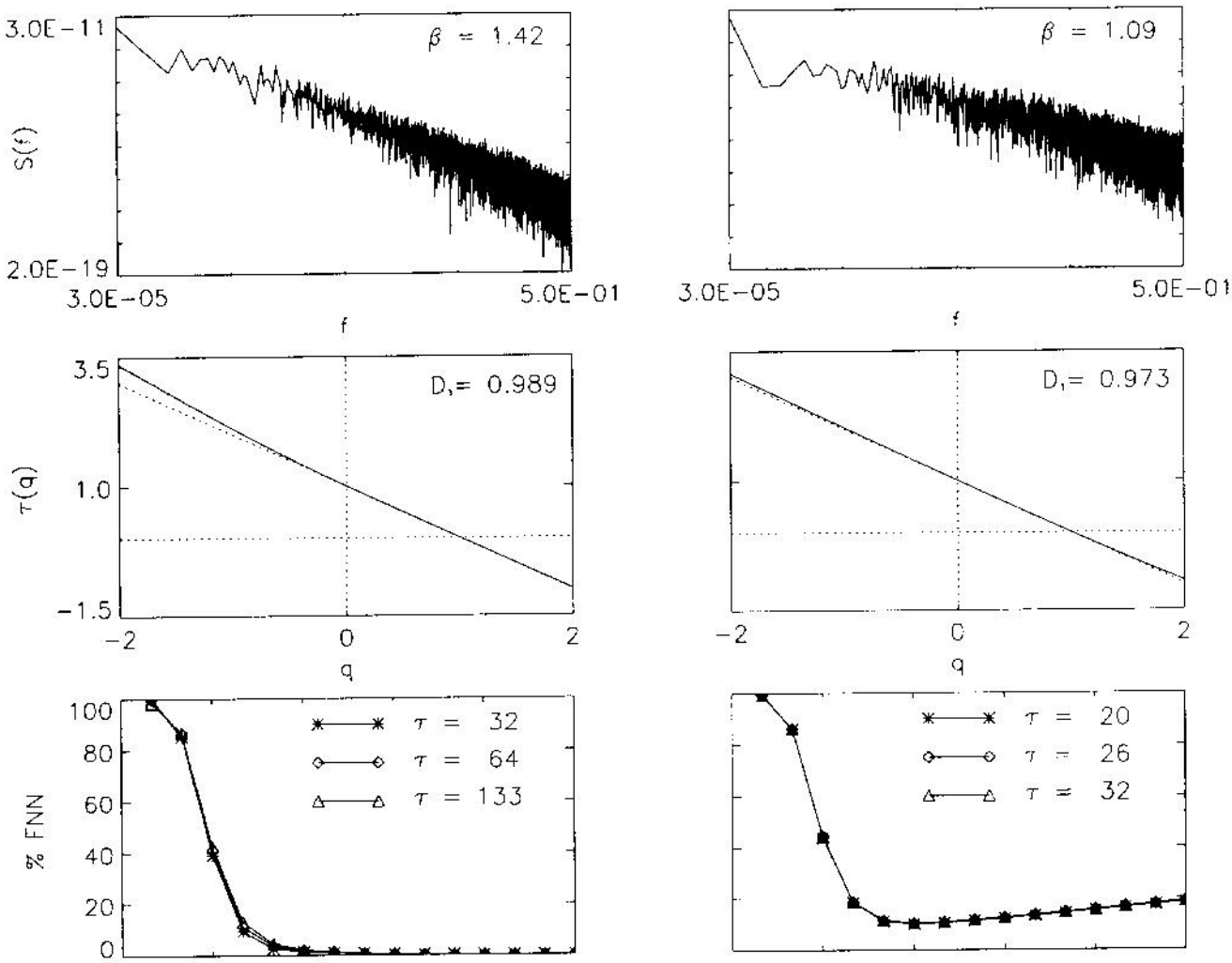

Fig. 2 Sample statistics for deterministic FM measures $DY1$ and $DY2$: (i) Power spectrum, $S(f) \sim f^{-\beta}$; (ii) Mass exponents, $\tau(q)$; and (iii) Percentage of false neighbors, $\%FNN$, for alternative delays, τ, as a function of embedding dimension, m.

their power spectrum (over four cycles), and yield a $1/f^{\beta}$ noise ($\beta = 1.42$) for $DY1$ and a more irregular $1/f$ noise ($\beta = 1.09$) for $DY2$. As depicted in the middle of Fig. 2, these trends are also noticed while comparing the mass exponent plots for both sets (i.e. the scalings $\tau(q)$ of sums of a measure raised to a power q). Observe, in particular, the alternative entropy dimensions obtained for the two sets (0.989 and 0.973, respectively) that confirm that $DY2$ is more "disorganized" than $DY1$.

The aforementioned trends remain when calculating the necessary number of lags for phase-space reconstructions as reported before, for the fact that $DY2$ is more irregular than $DY1$ is reflected in a smaller of lags: 26 versus 245 to the first local minimum of the autocorrelation function, 472 versus 4860 to a correlation equal to e^{-1}, and 20 versus 133 to the first local minimum of the mutual information function.

As shown in the bottom of Fig. 2, the dynamical behavior of the two measures, as quantified by the percentage of false near neighbors of successive embeddings for dimensions up to 15, turns out to be quite distinct. On the one hand, and surprisingly, $DY1$ yields a behavior that fully unfolds at low dimension m that equals 5 or 6, for delays τ that include the one defined by the mutual information analysis (i.e. 133) and two others below (i.e. 32 and 64). On the other hand, and also surprisingly, the percentage of false near neighbors for $DY2$ neither reaches zero nor remains stable (after reaching the minimum of about 10%), indicating that for delays defined by the first local minima of the mutual information and autocorrelation functions (i.e. 20

and 26), and also for $\tau = 32$, such a measure does not unfold and therefore may be classified as high-dimensional.

As the largest Lyapunov exponents analysis for the two measures, employing all alternate reconstructed attractors, yield positive values, indicating sensitivity to initial conditions, these results suggest that the deterministic measure $DY1$ may be considered as the outcome of a dynamical process that is low-dimensional and chaotic, while $DY2$ (also deterministic by construction) may be termed high-dimensional and stochastic.

5. DYNAMICAL PROPERTIES OF OTHER DERIVED MEASURES

As the results just reported are intriguing, given the deterministic nature of the analyzed sets, this section presents a sensitivity analysis aimed at identifying general dynamic conditions for other FM-generated measures. As the results clearly depend on the amount of filtering performed by an FIF, such analysis includes varying the scalings of the relevant affine mappings [Eq. (1)] and hence the fractal dimensions of graphs of such fractal functions.

To this effect, another 64 FM-derived measures were generated, 32 coming from fractal functions whose graphs have fractal dimensions greater than 1 and the remaining 32 from functions whose graphs have fractal dimensions equal to 1. To keep the analysis manageable, all the new measures were generated over the y-axis (i.e. maintained $\theta = 0°$), had the same data size as that of $DY1$ and $DY2$ (i.e. 65 536 values), used the same parent binomial multifractal measure DX as before ($p_1 = 0.6$, $p_2 = 0.4$), and came from FIF that pass by the same set of three points $\{(0, 0), (0.5, 1.0)$ and $(1, 0)\}$.

These two groups of measures, shown in Figs. 3 and 4 respectively, were obtained using the FM parameters presented in Tables 1 and 2, and include all different sign combinations on the scalings d_1 and d_2, namely case 1: both positive; case 2: positive, negative; case 3: negative, positive; and case 4: both negative. As presented in Tables 1 and 2 (fourth column), the first group of measures (Fig. 3) uses fractal functions whose graphs have fractal dimensions (D) between 1.263 and 1.485, while the second group (Fig. 4) employs FIF, whose graphs' dimension equals 1.

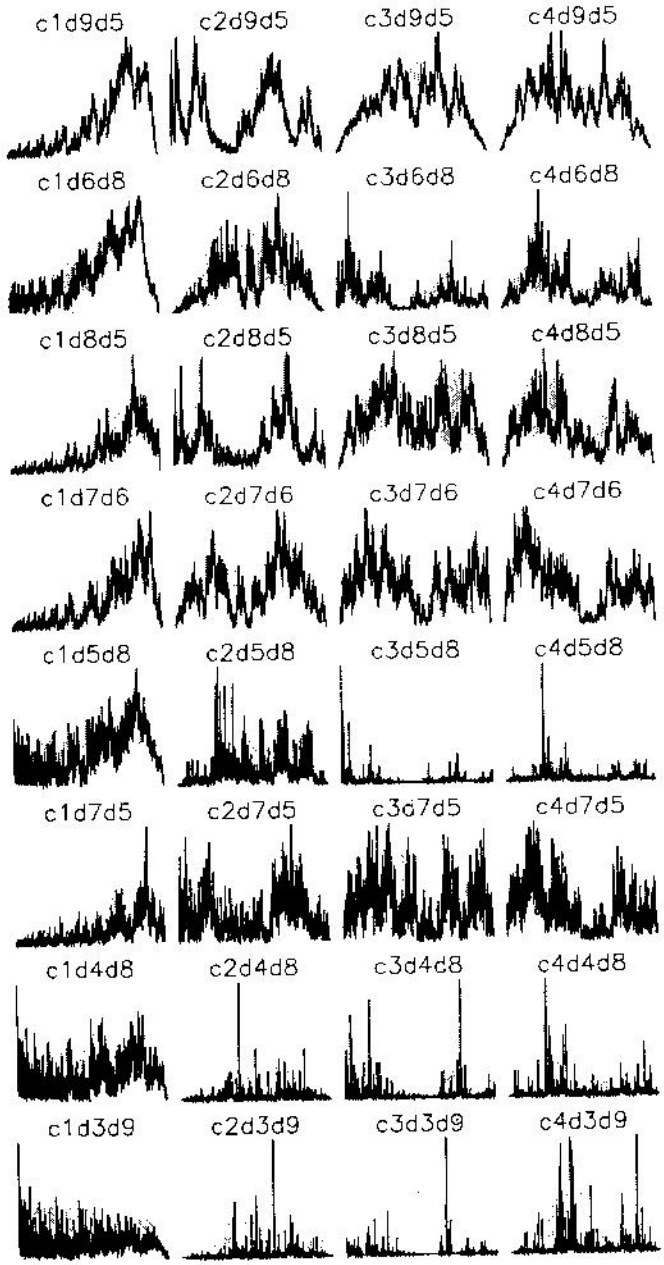

Fig. 3 FM derived measures as defined in Table 1.

As can be seen in the first column of Figs. 3 and 4 (i.e. for d_1 and d_2 both positive), and in consonance with the results presented for $DY1$ and $DY2$ (sixth row of Fig. 3 and seventh row of Fig. 4), measures associated with higher fractal dimensions (Fig. 3) contain many positive values and are typically more correlated and less intermittent than the others (Fig. 4).

These trends, although maintained in most sign combination cases on the affine mapping scalings, are not fully consistent for there are few instances

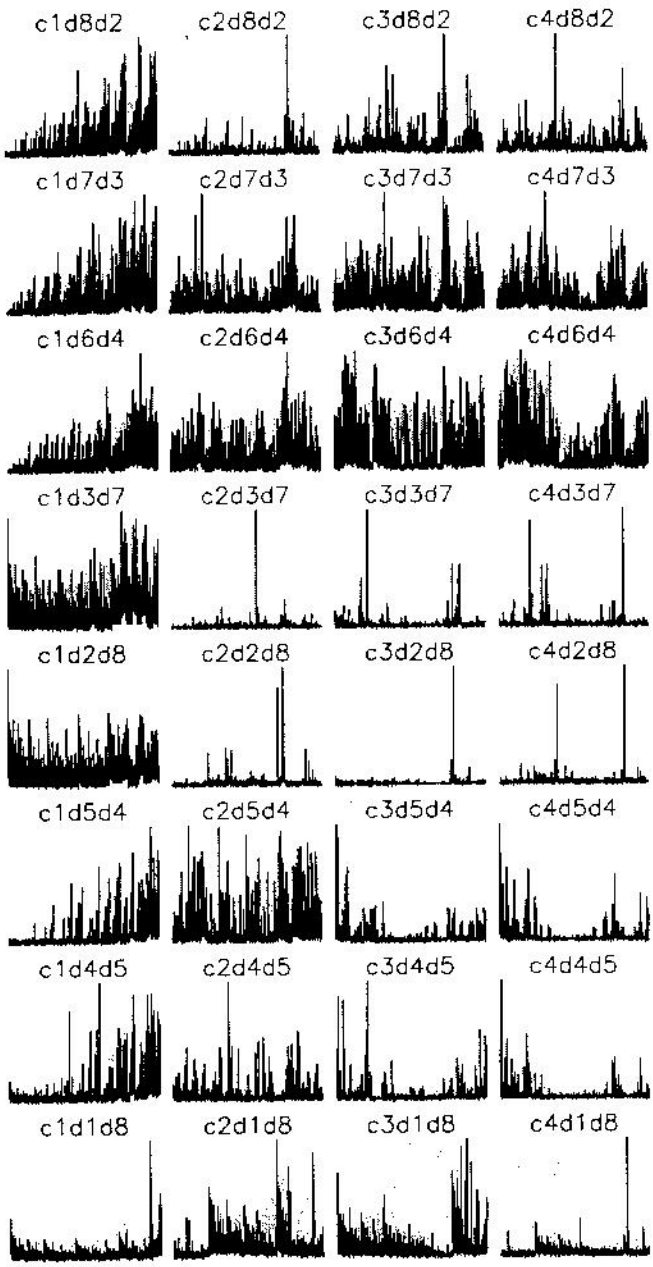

Fig. 4 FM derived measures as defined in Table 2.

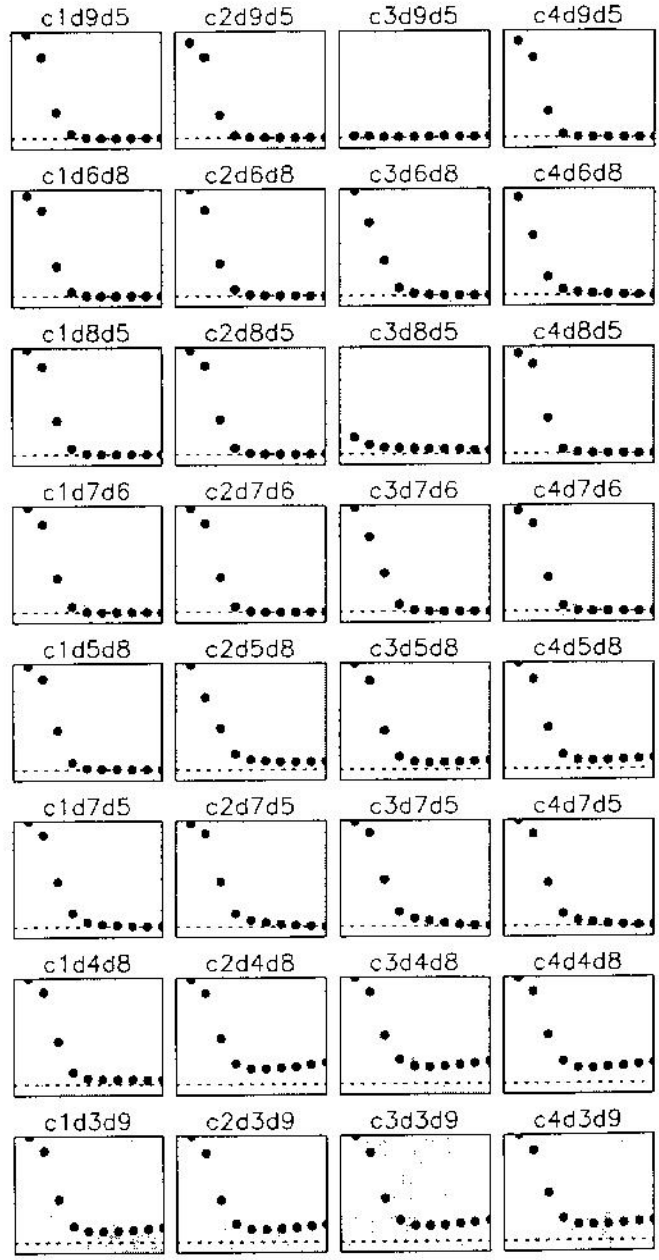

Fig. 5 Power spectrum, $S(f) \sim f^{-\beta}$, for measures in Fig. 3. Log-log axis have horizontal and vertical scales of $[1.0e-5,\ 1.0e-0]$ and $[1.0e-19,\ 1.0e-11]$, respectively.

in Fig. 3 (i.e. fifth row, columns three and four; and seventh and eighth rows, columns two to four) and in Fig. 4 (e.g. fourth and fifth rows, columns two to four) that are dominated by few large peaks. These happen because the dimension of the graph of an FIF alone (for the cases shown) does not define completely the nature of the derived measure. For instance, the set on the fifth row and third column in Fig. 3 shows a measure dominated by few peaks because the skew in DX (i.e. higher on the left) is "canceled" by the down-up notion of the fractal function (i.e. $d_1 = -0.5$, $d_2 = 0.8$).

Figures 5 and 6 show that all sets in Figs. 3 and 4 exhibit power scaling in their power spectra, although some sets exhibit better linear fits than others. Even though there is no one-to-one relationship between the relevant scaling exponent β (calculated via a regression based on the last half of the values) and a given combination on FM scalings, notice that the overall trends encountered earlier with $DY1$ and $DY2$ remain. For the spectra in both figures reflect the general nature of the derived measures and

Table 1 Scaling parameters, d_1 and d_2, dimensions of graphs of fractal interpolating functions, D, first local minimum of autocorrelation function, $\rho(flm)$, decay time to e^{-1} on autocorrelation, $\rho(e^{-1})$, first local minimum of average mutual information function, $I(flm)$, and entropy dimension of derived measures, $(D_1)_{DY}$, for sets in Fig. 3.

Set	d_1	d_2	D	$\rho(flm)$	$\rho(e^{-1})$	$I(flm)$	$(D_1)_{DY}$
c1d9d5	0.9	0.5	1.485	16384	11501	282	0.998
c2d9d5	0.9	−0.5	1.485	7758	3675	267	0.998
c3d9d5	−0.9	0.5	1.485	5279	3529	343	0.999
c4d9d5	−0.9	−0.5	1.485	3239	2604	226	0.999
c1d6d8	0.6	0.8	1.485	8289	10096	219	0.998
c2d6d8	0.6	−0.8	1.485	2323	5912	136	0.997
c3d6d8	−0.6	0.8	1.485	307	3950	168	0.995
c4d6d8	−0.6	−0.8	1.485	340	3902	205	0.996
c1d8d5	0.8	0.5	1.378	845	9626	230	0.996
c2d8d5	0.8	−0.5	1.378	941	2990	194	0.997
c3d8d5	−0.8	0.5	1.378	1662	2118	231	0.998
c4d8d5	−0.8	−0.5	1.378	796	2468	181	0.997
c1d7d6	0.7	0.6	1.378	1655	11037	112	0.996
c2d7d6	0.7	−0.6	1.378	1712	3386	265	0.997
c3d7d6	−0.7	0.6	1.378	1433	2507	165	0.997
c4d7d6	−0.7	−0.6	1.378	1077	6282	217	0.997
c1d5d8	0.5	0.8	1.378	215	7347	109	0.994
c2d5d8	0.5	−0.8	1.378	98	1814	70	0.986
c3d5d8	−0.5	0.8	1.378	10	265	12	0.969
c4d5d8	−0.5	−0.8	1.378	6	601	36	0.975
c1d7d5	0.7	0.5	1.263	245	4860	133	0.989
c2d7d5	0.7	−0.5	1.263	210	2489	120	0.990
c3d7d5	−0.7	0.5	1.263	486	1488	165	0.991
c4d7d5	−0.7	−0.5	1.263	213	4079	129	0.992
c1d4d8	0.4	0.8	1.263	39	5388	37	0.990
c2d4d8	0.4	−0.8	1.263	18	126	34	0.969
c3d4d8	−0.4	0.8	1.263	16	63	63	0.934
c4d4d8	−0.4	−0.8	1.263	32	159	41	0.955
c1d3d9	0.3	0.9	1.263	9	248	9	0.987
c2d3d9	0.3	−0.9	1.263	12	79	35	0.968
c3d3d9	−0.3	0.9	1.263	8	75	22	0.929
c4d3d9	−0.3	−0.9	1.263	22	113	61	0.954

hence give larger exponents when sets are produced by fractal functions whose graphs have dimensions greater than one. Overall, sets in Fig. 3, except possibly those dominated by few large peaks, may be termed as "pink noises" $(1/f^{\beta})$, whereas those in Fig. 4 may be described as "$1/f$ noises."

Tables 1 and 2, in their fifth, sixth and seventh columns, include information regarding delay times as defined from the autocorrelation function (i.e. $\rho(flm)$, $\rho(e^{-1})$) and mutual information function (i.e. $I(flm)$). As may be seen, most measures in Fig. 3 (except those dominated by few peaks)

Table 2 Scaling parameters, d_1 and d_2, dimensions of graphs of fractal interpolating functions, D, first local minimum of autocorrelation function, $\rho(flm)$, decay time to e^{-1} on autocorrelation, $\rho(e^{-1})$, first local minimum of average mutual information function, $I(flm)$, and entropy dimension of derived measures, $(D_1)_{DY}$, for sets in Fig. 4.

Set	d_1	d_2	D	$\rho(flm)$	$\rho(e^{-1})$	$I(flm)$	$(D_1)_{DY}$
c1d8d2	0.8	0.2	1	9	867	3	0.955
c2d8d2	0.8	−0.2	1	25	132	37	0.961
c3d8d2	−0.8	0.2	1	19	148	65	0.970
c4d8d2	−0.8	−0.2	1	21	77	48	0.970
c1d7d3	0.7	0.3	1	3	366	8	0.955
c2d7d3	0.7	−0.3	1	43	486	58	0.962
c3d7d3	−0.7	0.3	1	23	255	56	0.966
c4d7d3	−0.7	−0.3	1	63	156	43	0.963
c1d6d4	0.6	0.4	1	7	2250	4	0.965
c2d6d4	0.6	−0.4	1	59	599	32	0.963
c3d6d4	−0.6	0.4	1	46	227	30	0.956
c4d6d4	−0.6	−0.4	1	51	771	26	0.960
c1d3d7	0.3	0.7	1	11	4568	5	0.981
c2d3d7	0.3	−0.7	1	4	27	16	0.965
c3d3d7	−0.3	0.7	1	18	82	25	0.945
c4d3d7	−0.3	−0.7	1	7	46	29	0.957
c1d2d8	0.2	0.8	1	3	814	3	0.980
c2d2d8	0.2	−0.8	1	13	125	13	0.970
c3d2d8	−0.2	0.8	1	7	15	7	0.952
c4d2d8	−0.2	−0.8	1	18	35	7	0.963
c1d5d4	0.5	0.4	1	26	420	39	0.971
c2d5d4	0.5	−0.4	1	32	79	59	0.957
c3d5d4	−0.5	0.4	1	6	29	21	0.938
c4d5d4	−0.5	−0.4	1	9	170	16	0.952
c1d4d5	0.4	0.5	1	26	432	20	0.973
c2d4d5	0.4	−0.5	1	28	39	21	0.958
c3d4d5	−0.4	0.5	1	18	45	66	0.942
c4d4d5	−0.4	−0.5	1	6	173	29	0.959
c1d1d8	0.1	0.8	1	6	96	6	0.972
c1d1d8	0.1	−0.8	1	6	283	14	0.980
c1d1d8	−0.1	0.8	1	7	207	4	0.970
c1d1d8	−0.1	−0.8	1	9	172	4	0.978

exhibit indeed larger correlation lengths and larger delays to the first local minimum of the mutual information function than those in Fig. 4. These overall trends are confirmed by the measures' entropy dimensions, $(D_1)_{DY}$, as reported on the last column of Tables 1 and 2. Notice that the correlated measures in Fig. 3 give values close to the measures' support, i.e. one, and that the very noisy ones in Fig. 4 and those dominated by few large peaks in Figs. 3 and 4 give dimensions smaller than one.

Figures 7 and 8 summarize the analysis of false near neighbors, up to ten embedding dimensions

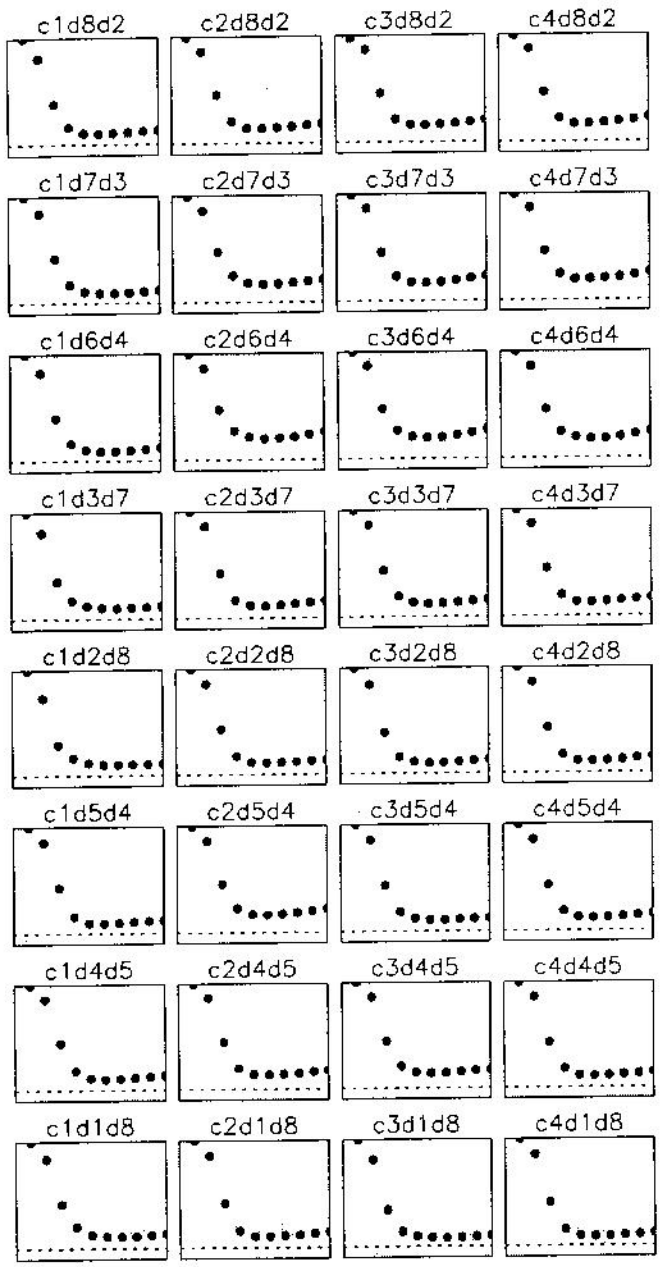

Fig. 6 Power spectrum, $S(f) \sim f^{-\beta}$, for measures in Fig. 4. Log-log axis have horizontal and vertical scales of $[1.0e-5, 1.0e-0]$ and $[1.0e-19, 1.0e-11]$, respectively.

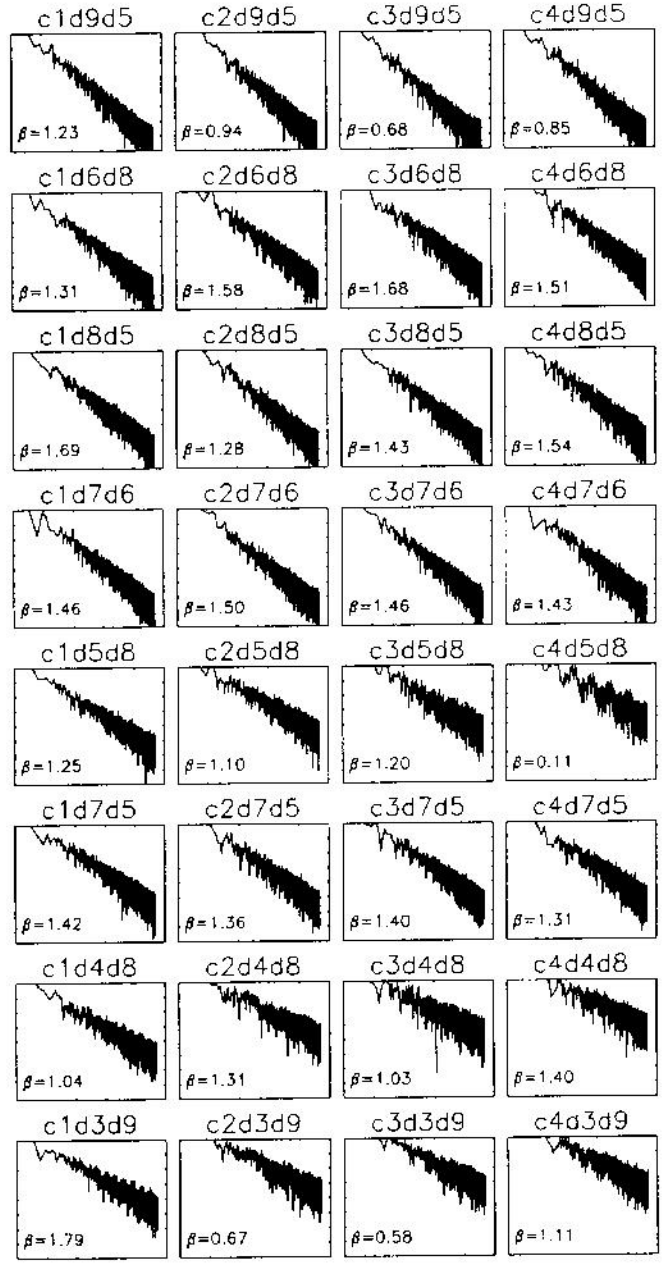

Fig. 7 Percentage of false neighbors, $\%FNN$, as a function of embedding dimension, m, for measures in Fig. 3. The horizontal and vertical scales are $[0, 10]$ and $[-10, 100]$, respectively.

and using the delay as defined from the mutual information function, performed on both groups of sets in an attempt to classify their inherent dynamics. As is seen, the more correlated measures in Fig. 3 result in stable low-dimensional unfoldings having four, five or six coordinates (Fig. 7). On the other hand, those more erratic sets, that are either highly uncorrelated or dominated by few large peaks in Figs. 3 and 4, do not show stabilization on the percentage of false near neighbors (Fig. 8), and then may be termed dynamically high-dimensional. Notice that these observations are in agreement with the aforementioned analysis pertaining to Tables 1 and 2. As Lyapunov exponent calculations (not presented here) suggest that the analyzed measures yield sensitivity to initial conditions, these results confirm that the FM approach may be used to simulate both chaotic and stochastic signals.

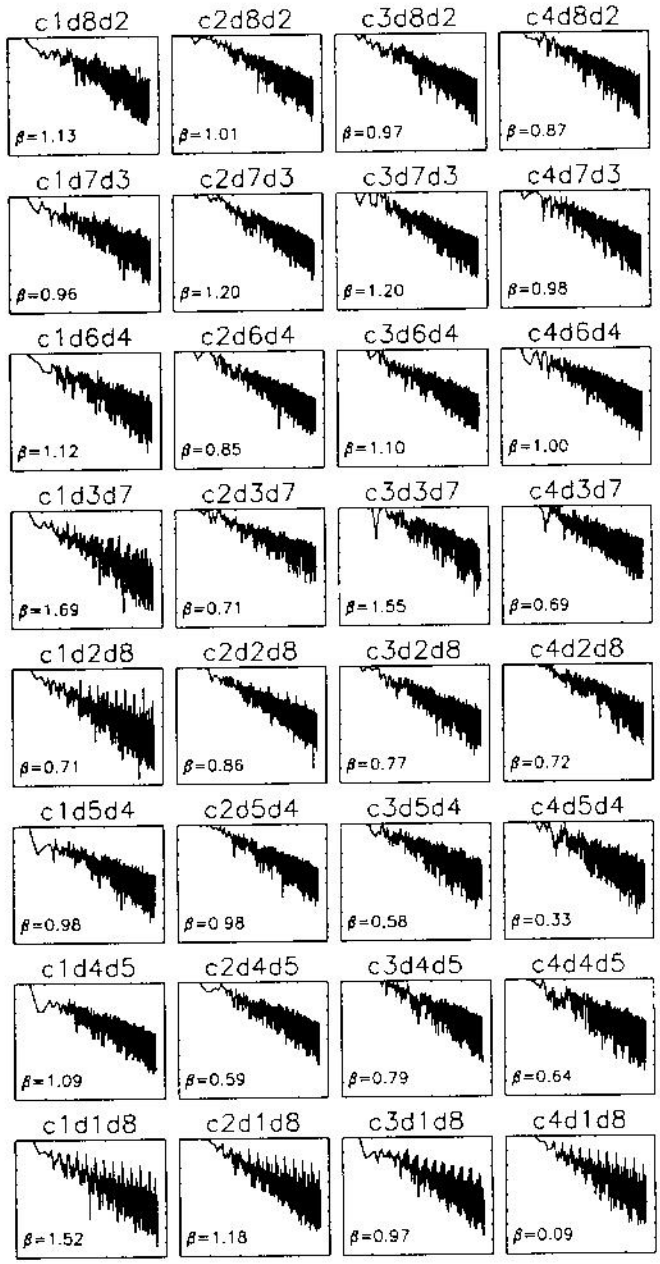

Fig. 8 Percentage of false neighbors, $\%FNN$, as a function of embedding dimension, m, for measures in Fig. 4. The horizontal and vertical scales are $[0, 10]$ and $[-10, 100]$, respectively.

It is worth remarking that the minimal number of embedding dimensions found for the deterministic sets in Figs. 3 and 4 are, in general, related to the observation that stochastic processes with $1/f^{\beta}$ power spectra may define such minimal dimensions via saturation in correlation dimension calculations, i.e. $d = 2/(\beta - 1)$.[8] Notice, for instance, that $DY1$ and $DY2$, having β values of 1.42 and 1.09, respectively, yield d values of 4.76 and 22.2 that indeed capture the low- and high-dimensionality of those sets, but, as there is ample variability on β values in Figs. 5 and 6 (with several values less than one), no general conclusions may be drawn.

6. CONCLUSIONS

It has been illustrated that the FM methodology, a deterministic geometric procedure aimed at representing complex positive time series wholistically as projections of multifractal measures supported by the graphs of FIF, produces a host of $1/f^{\beta}$ multifractal noises possessing varied textures and appearances, whose dynamic behavior may be classified, depending on FM parameters and mutual information calculations, as low-dimensional and "chaotic" or high-dimensional and "stochastic." These findings, apparently contradictory given the deterministic nature of the FM representation, support the vision that the concept of projections may be a suitable alternative in the study of a variety of natural records.

7. ACKNOWLEDGMENTS

The work presented in this article was supported in part by the USEPA via Grant GAD # R824780 and by NASA under Grant NAG5-7441.

REFERENCES

1. C. E. Puente and N. Obregón, "A Deterministic Geometric Representation of Temporal Rainfall: Results for a Storm in Boston," *Water Resour. Res.* **32**(9), 2825 (1996).
2. C. E. Puente and N. Obregón, "A Geometric Platonic Approach to Multifractality and Turbulence," *Fractals* **7**(4), 403 (1999).
3. C. E. Puente, N. Obregón, O. Robayo, M. G. Puente and D. Simsek, "Projections Off Fractal Functions: A New Vision of Nature's Complexity," *Fractals* **7**(4), 387 (1999).
4. N. Obregón, B. Sivakumar and C. E. Puente, "A Deterministic Geometric Representation of Temporal Rainfall: Sensitivity Analysis for a Storm in Boston," *Water Resour. Res.*, submitted (2001a).
5. N. Obregón, C. E. Puente and B. Sivakumar, "Modeling High Resolution Rain Rates via a Deterministic Fractal-Multifractal Approach," *Fractals*, submitted (2001b).
6. C. E. Puente, O. Robayo, M. C. Diaz and B. Sivakumar, "A Fractal-Multifractal Approach to

Groundwater Contamination. I. Modeling Conservative Tracers at the Borden Site," *Stoch. Env. Res. Risk Assess.* **15**(5), in press (2001a).
7. C. E. Puente, O. Robayo and B. Sivakumar, "A Fractal-Multifractal Approach to Groundwater Contamination. II. Predicting Conservative Tracers at the Borden Site," *Stoch. Env. Res. Risk Assess.* **15**(5), in press (2001b).
8. A. R. Osborne and A. Provenzale, "Finite Correlation Dimension for Stochastic Systems with Power-Law Spectra," *Physica* **D35**, 357 (1989).
9. C. E. Puente, "Multinomial Multifractals, Fractal Interpolators, and the Gaussian Distribution," *Phys. Lett.* **A161**, 441 (1992).
10. C. E. Puente, "Deterministic Fractal Geometry and Probability," *Int. J. Bifurc. Chaos* **4**(6), 1613 (1994).
11. B. B. Mandelbrot, "Multifractal Measures Especially for the Geophysicist," in *Fractals in Geophysics*, eds. C. H. Scholz and B. B. Mandelbrot (Birkhauser Verlag, Basel, 1989), pp. 1–42.
12. M. F. Barnsley, "Fractal Functions and Interpolation," *Constr. Approx.* **2**, 302 (1986).
13. M. F. Barnsley, *Fractals Everywhere* (Academic Press, 1988).
14. C. Meneveau and K. R. Sreenivasan, "Simple Multifractal Cascade Model for Fully Developed Turbulence," *Phys. Rev. Lett.* **59**, 1424 (1987).
15. K. R. Sreenivasan, "Fractals and Multifractals in Fluid Turbulence," *Ann. Rev. Fluid Mech.* **23**, 539 (1991).
16. S. Lovejoy and D. Schertzer, "Multifractals, Universality Classes and Satellite and Radar Measurements of Cloud and Rain Fields," *J. Geophys. Res.* **95**, 2021 (1990).
17. Y. Tessier, S. Lovejoy and D. Schertzer, "Universal Multifractals: Theory and Observations for Rain and Clouds," *J. Appl. Meteorol.* **2**, 223 (1993).
18. N. H. Packard, J. P. Crutchfield, J. D. Farmer and R. S. Shaw, "Geometry from a Time Series," *Phys. Rev. Lett.* **45**(9), 712 (1980).
19. F. Takens, "Detecting Strange Attractors in Turbulence," in *Dynamical Systems and Turbulence*, eds. D. A. Rand and L. S. Young (Lecture Notes in Mathematics 898, Springer-Verlag, Berlin, 1981), pp. 366–381.
20. J. Holzfuss and G. Mayer-Kress, "An Approach to Error-Estimation in the Application of Dimension Algorithms," in *Dimensions and Entropies in Chaotic Systems*, ed. G. Mayer-Kress (Springer-Verlag, New York, 1986), pp. 114–122.
21. A. M. Frazer and H. L. Swinney, "Independent Coordinates for Strange Attractors from Mutual Information," *Phys. Rev.* **A33**(2), 1134 (1986).
22. A. A. Tsonis and J. B. Elsner, "The Weather Attractor over Very Short Timescales," *Nature* **333**, 545 (1988).
23. M. B. Kennel, R. Brown and H. D. I. Abarbanel, "Determining Minimum Embedding Dimension Using a Geometrical Construction," *Phys. Rev.* **A45**, 3403 (1992).
24. H. D. I. Abarbanel, *Analysis of Observed Chaotic Data* (Springer-Verlag, New York, 1996).
25. J. W. Havstad and C. L. Ehlers, "Attractor Dimension of Nonstationary Dynamical Systems from Small Data Sets," *Phys. Rev.* **A39**(2), 845 (1989).